Conformational transitions induced in heparin octasaccharides by binding with antithrombin III

Marco Guerrini, Sara Guglieri, Daniela Beccati, Giangiacomo Torri, Christian Viskov, Pierre Mourier

Biochemical Journal Immediate Publication. Published on 23 Jun 2006 as manuscript BJ20060656

Conformational transitions induced in heparin octasaccharides by binding with antithrombin III.

Marco GUERRINI[§], Sara GUGLIERI[§], Daniela BECCATI[§], Giangiacomo TORRI[§], Christian VISKOV[&] and Pierre MOURIER[&]

[§] "G. Ronzoni" Institute for Chemical and Biochemical Research, via G. Colombo 81, 20133 Milan, Italy. [&] Sanofi-Aventis, 13 Quai Jules Guesde, 94403 Vitry sur Seine, France.

* Correspondence to Dr Marco Guerrini, G. Ronzoni Institute for Chemical and Biochemical Research, G. Colombo 81, 20133 Milan, Italy. Phone: (+39) 02 – 7064 1627. Fax: (+39) 02 – 7064 1634. E-mail: guerrini@ronzoni.it

ABSTRACT:

The present study deals with the conformation in solution of two heparin octasaccharides containing the pentasaccharide sequence $GlcN_{NAc,6S}$- GlcA- $GlcN_{NS,3,6S}$- $IdoA_{2S}$- $GlcN_{NS,6S}$ (AGA*IA) located at different positions in the heparin chain and focuses on establishing geometries of IdoA residues ($IdoA_{2S}$ and IdoA) both inside and outside the AGA*IA sequence. AGA*IA constitutes the active site for antithrombin (AT) and is essential for the expression of high anticoagulant and antithrombotic activities. Analysis of NMR parameters (NOEs, transferred NOEs and coupling constants) for the two octasaccharides indicated that between the $^1C_4$ and $^2S_0$ conformations present in dynamic equilibrium in the free state for the $IdoA_{2S}$ residue within AGA*IA, AT selects the $^2S_0$ form, as previously shown [Hricovini, Guerrini, Bisio, Torri, Petitou and Casu (2001) Biochem. J. **359**, 265-272]. Notably, the $^2S_0$ conformation is also adopted by the non-sulfated IdoA residue preceding AGA*IA which, in the absence of AT, adopts predominantly the $^1C_4$ form. These results further support the concept that heparin-binding proteins influence the conformational equilibrium of iduronate residues that are directly or indirectly involved in binding and select one of their equi-energetic conformations for best fitting in the complex. The complete reversal of an iduronate conformation preferred in the free-state is also demonstrated for the first time. Preliminary docking studies provided information on the octasaccharide binding location agreeing most closely with the experimental data. These results suggest a possible biological role for the non-sulfated IdoA residue preceding AGA*IA, previously thought not to influence the AT-binding properties of the pentasacchride. Thus, for each AT binding sequence longer than AGA*IA, the interactions with the protein could differ and give to each heparin fragment a specific biological response.

KEYWORDS

antithrombin; conformation; docking; heparin; NMR spectroscopy; protein-carbohydrate interaction.

ABBREVIATIONS

GAGs, glycosaminoglycans; GlcN, α-D-glucosamine; $GlcN_{NAc,6S}$, N-acetylated,6-O-sulfated α-D-glucosamine; $GlcN_{NS,6S}$, N,6-O-disulfated α-D-glucosamine; $GlcN_{NS,3,6S}$ N,3,6-O-trisulfated α-D-glucosamine; IdoA, α-L-iduronic-acid; $IdoA_{2S}$, 2-O-sulfated α-L-iduronic-acid; GlcA, β-D-glucuronic acid; AGA*IA, pentasaccharide sequence of $GlcN_{NAc,6S}$- GlcA- $GlcN_{NS,3,6S}$- $IdoA_{2S}$- $GlcN_{NS,6S}$; ΔU, 4,5-unsaturated uronic acid; ΔU_{2S}, 2-O-sulfated,4,5-unsaturated uronic acid AT, antithrombin; 3D, three-dimensional; NOE, nuclear Overhauser effect; tr-NOE transferred nuclear

Overhauser effect ; NOESY, NOE spectroscopy; CTA-SAX, cetyltrimethylammonium-strong anion exchange, DQF-COSY, double quantum filter correlation spectroscopy; TOCSY total correlation spectroscopy; $^{3}J_{H-H}$, three bond proton-proton coupling constants; GPC, gel permeation chromatography; GA-LS, genetic algorithm/local search.

RUNNING TITLE

Heparin octasaccharides-AT interaction**.**

Biochemical Journal Immediate Publication. Published on 23 Jun 2006 as manuscript BJ20060656

INTRODUCTION

Heparin is a sulfated glycosaminoglycan consisting predominantly of repeating disaccharide units of α-1,4-linked 2-O-sulfated L-iduronic acid ($IdoA_{2S}$) and N-sulfated,6-O-sulfated D-glucosamine ($GlcN_{NS,6S}$). "Irregular" sequences containing N-acetyl D-glucosamine ($GlcN_{NAc}$) and β-D-glucuronic acid (GlcA), as well as other under-sulfated residues, also contribute to other biological activities of heparin. The unique pentasaccharide domain AGA*IA ($GlcN_{NAc,6S}$-GlcA-$GlcN_{NS,3,6S}$-$IdoA_{2S}$-$GlcN_{NS,6S}$), which constitutes the active site for antithrombin (AT), is essential for the anticoagulant and antithrombotic activities of heparin [1-2].

The interaction of AT with active heparin oligosaccharides induces the elongation of the helix D of the protein through a conformational change in its reactive centre loop. In the latent conformation, three of the binding residues located in this helix are hydrogen-bonded to other regions of the molecule. In the active conformation, the side chains of the most important binding residues are not involved in hydrogen bonding and are therefore available to form ionic interactions with the heparin saccharides [3-4]. Stabilization of the AT active conformation, induced through binding with the pentasaccharide, results in a 300 fold acceleration in the rate of factor Xa inactivation [5].

Understanding the interaction between AT and AGA*IA containing heparin oligosaccharides at the molecular level requires detailed knowledge of the three-dimensional (3D) structure of both partners in the complex. In this view conformational studies of complexes between the AT and synthetic AGA*IA and AGA*IA structural variants have been elucidated recently by both crystallography and NMR studies [6-8]. The majority of such studies focus on describing the structural details of AT, while conformations of the oligosaccharides in the bound state have not been extensively studied. Nevertheless, reference values describing ligand geometries can be derived from the Protein Data Bank (pdb) files of the complexes. Despite their structural differences, all heparin oligosaccharides analysed in the above studies adopt similar glycosidic linkage geometries and residue conformations, supporting the idea that the AGA*IA sequence binds AT in a structurally well-defined manner.

NMR methodologies permitting the determination of both free and bound structures have been widely described [9-11]. Such approaches are essentially based on the nuclear Overhauser effect (NOE) and transferred NOEs (tr-NOE) together with scalar coupling constant analyses. NOE magnitudes, which depend on inter-proton distances, are commonly used to study the glycosidic linkage geometries of GAGs [12]. Moreover, together with inter-proton coupling constants, NOEs provide information on α L-iduronic acid (IdoA) ring geometries, which possess an unusual degree of flexibility. Indeed, it was demonstrated that α L-IdoA and $IdoA_{2S}$ can adopt three different equi-

energetic conformations in dynamic equilibrium: $^1C_4$, $^4C_1$, and $^2S_0$ (Fig. 1) [13]. When this residue comprises part of heparin and heparin-like molecules in solution, the relative populations of such conformers vary depending on whether the adjacent residues are sulfated [14]. The conformational equilibrium may also be affected by external factors such as ionic strength and specific counterions [15-16]. Even if the overall geometry of the heparin helical chain is not dramatically influenced by the IdoA conformations, the spacing between sulfate groups on adjacent residues is consistently different for the two prevalent local conformations ($^1C_4$ and $^2S_0$) and the sulfate groups cluster in different ways along the chain axis [17]. The "plasticity" of IdoA residues has also been proposed to facilitate the most effective docking of anionic groups of GAGs to the appropriate basic groups of proteins [16, 18]. Analysis of a large number of heparin oligosaccharide-protein complexes has led to the general concept that the linear propagation of GAG chains is interrupted at the binding site level by "kinks" associated with a conformation of an iduronic acid different from that prevailing in the portion of chain not involved in the binding [19].

Both NMR and X-ray studies of the AT-AGA*IA complex revealed that the $IdoA_{2S}$ residue of the pentasaccharide assumes the $^2S_0$ conformation when bound to the protein [6, 8]. However, this group is not involved in any dipolar contact with protein residues. Indeed, the 2-OSO_3 group of the iduronic acid residue appears to be the main driving force in affecting the shift of the conformational equilibrium of $IdoA_{2S}$ towards the skew-boat form, thus enhancing dipolar contacts between the AGA*IA reducing disaccharides with some basic amino acids [8].

Extension of the AGA*IA chain towards either its reducing or non-reducing ends is thought to play a role in the binding and activation of AT. The knowledge of such roles is particularly important in the design of "tailored" low and very low molecular weight heparins with an accurate prediction of their anti-Xa and anti-IIa activities and thus in understanding the *in-vivo* behaviour of complex mixtures of AT binding sites present in low molecular weight heparin (LMWH) samples. Although several studies have been carried out on complexes of AT with different AGA*IA-containing fragments, their roles are still not clear because of a lack of appropriate experimental models and compounds [20-22].

The present work deals with NMR and molecular docking studies of the conformational and AT-binding properties of two naturally occurring AGA*IA-containing octasaccharides. It allowed the influence of disaccharide extensions at the reducing or non-reducing end of the active pentasaccharide sequence to be investigated. Octasaccharides **A** and **B** were isolated from Lovenox® (enoxaparin), a low molecular weight heparin obtained by β-eliminative cleavage of a porcine mucosal heparin. Accordingly they contain N-acetyl glucosamine as the first residue of the AGA*IA sequence (as in the original heparin) instead of an N-sulfated glucosamine (as in the most

extensively studied synthetic pentasaccharides). Octasaccharide **A** and **B** have the following primary structures, respectively: ΔU-GlcN$_{NAc,6S}$-GlcA-GlcN$_{NS,3,6S}$-IdoA$_{2S}$*-GlcN$_{NS,6S}$-IdoA$_{2S}$-GlcN$_{NS,6S}$ and ΔU$_{2S}$-GlcN$_{NS,6S}$-IdoA-GlcN$_{NAc,6S}$-GlcA-GlcN$_{NS,3,6S}$-IdoA$_{2S}$*-GlcN$_{NS,6S}$, where ΔU corresponds to the 4,5 unsaturated uronate residue arising from β-eliminative cleavage.

To investigate how binding to AT affects the octasaccharide conformations, we paid particular attention to the geometry of iduronic acid residues, both inside (IdoA$_{2S}$*) and outside the AGA*IA sequence (IdoA$_{2S,}$ and IdoA). An AT-induced drive towards the $^2S_0$ conformation of the IdoA$_{2S}$* residue within the AGA*IA sequence was also observed when AGA*IA was part of both octasaccharides. Interestingly, an even stronger drive towards the $^2S_0$ conformation was observed for the non-sulfated iduronic acid preceding the AGA*IA sequence; a residue that was shown to be dispensable for high-affinity binding to AT [23]. Preliminary docking studies of both these molecules bound to AT were also carried out using the AutoDock 3.0 program [24]. Oligosaccharide conformations differently shifted through the AT binding site were thereby generated to identify the binding location that best agreed with the experimental data.

EXPERIMENTAL

Octasaccharides isolation and purification.

Octasaccharides **A** and **B** (Figures 2 and 3) were obtained by combining AT affinity chromatography and CTA-SAX anion exchange chromatography on a semi-preparative scale, starting from octasaccharide gel permeation chromatography (GPC) fractions of enoxaparin.

GPC of enoxaparin was performed on columns filled with ACA 202 gel (Sepracor) in $NaHCO_3$ 0.5M (100 x 5 cm). Selected fractions were neutralized with acetic acid and desalted on Sephadex G10 columns (100 x 7 cm). Then, the octasaccharide fraction (200 mg for each run) was chromatographed on an AT-sepharose column (40 x 5 cm). The column was prepared by coupling human AT (1g, hyphen Biomed) to cyanogen bromide activated sepharose 4B (Sigma). The methodology of Höök was used to prepare the AT column [25]. The low affinity portion was eluted from the column with 0.25 M NaCl solution buffered at pH 7.4 with 10mM TRIS. The high affinity octasaccharide fraction was eluted with 3M NaCl / TRIS 10 mM and desalted on Sephadex G10. The desired octasaccharides **A** and **B** were isolated using CTA-SAX chromatography. CTA-SAX semi-preparative columns were coated as described [26] on 250x 50mm or 250x22 mm columns filled with Hypersil BDS C_{18} 5µm or Hyperprep 100C_{18} 8µm. Briefly, column coating was performed as for the analytical columns, by percolating 1mM cetyl trimethylammonium hydrogensulfate solutions in H_2O-CH_3OH (68-32) v:v for 4h with the column temperature adjusted to 45°C. Mobile phases for oligosaccharide separations were aqueous sodium methanesulfonate

(Interchim) at concentrations varying between 0 and 2.5N. The pH was adjusted to 2.5 by addition of diluted methanesulfonic acid. Separations were achieved at 40°C. Salt concentration in the mobile phase was increased linearly from 0 to 2.5M over 60min. Flow rate was 40ml/min for 250x30mm columns and UV detection at 234 nm was used. Collected fractions were neutralized and desalted on Sephadex G10 after a preliminary treatment on Mega Bondelut C18 cartridges (Varian).

NMR samples preparation

All mono-dimensional and bi-dimensional NMR spectra were measured at 295K, at 600MHz with a Bruker Avance 600 spectrometer equipped with a high sensitivity 5mm TCI cryoprobe. For proton detection, 150µg octasaccharide samples (**A** and **B**) were dissolved in ^2H_2O (99.9%) and freeze dried to remove residual water. After exchanging the samples three times, samples were dissolved in 0.7 ml of 10 mM phosphate buffer 0.6 M NaCl; pH 7.4 with 3 mM EDTA in ^2H_2O (99.996%). For the binding studies, the two samples were prepared dissolving 1 mg of AT and 150µg of each octasaccharides **A** and **B** in the same phosphate buffer reaching a 1:3.5 AT:octasaccharide molar ratio.

Acquisition of NMR spectra

Proton spectra were recorded with presaturation of the residual water signal, with a recycle delay of 12s and 256 scans. Double quantum filter correlation spectroscopy (DQF-COSY) and total correlation spectroscopy (TOCSY) spectra were acquired using 32 scans per series of 2Kx512W data points with zero filling in F1 and a shifted squared cosine function was applied prior Fourier transformation. All nuclear Overhauser effect spectroscopy (NOESY) and transferred NOESY experiments were performed in a similar way. A total of 48 scans were collected for each free-induction decay (matrix 2048x 512 points) and data were zero-filled to 4Kx2K points before Fourier transformation. Mixing time values of 100 ms, 200 ms, and 300 ms were used.

Docking calculations

Docking calculations on octasaccharides **A** and **B** complexed with AT were performed by AutoDock program, version 3.0. The inhibitory chain of AT (X-ray structure pdb code 1AZX) [6] was used as a protein model. Kollman atomic partial charges were calculated with the AutoDockTools program. Octasaccharide models were built by using MACROMODEL program version 7.1. To evaluate the ability of our theoretical structures to interpret experimental data with

regard to the conformation adopted by iduronic acid moieties outside of AGA*IA sequence (IdoA and $IdoA_{2S}$), two models were used for each molecule, bearing such units; one in $^1C_4$ and the other in $^2S_0$ conformation. Their atomic partial charges were calculated by DivCon program version 4.0 [27]. A grid of probe atom interaction energies were computed first using the AutoGrid program; 37-Å side grids were used for all the ligands with a spacing of 0.375 Å. The ligand probes were then docked using Lamarckian genetic algorithm/local search GA-LS hybrid simulations. Rigid docking simulations were performed using 50 GA runs, and 500 generations for each run. Resulting ensembles of 50 conformations were then clustered using an rmsd tolerance of 0.5 Å. Output structures stored in trajectory files were visualized in AutoDockTools program. We wrote a specific Python script program to allow detection and systematic monitoring of contacts between side-chain polar groups of the protein and selected defined ligand atoms.

RESULTS AND DISCUSSION

The NMR spectra of the free octasaccharides were recorded in 0.6 M NaCl solution. The same NaCl concentration was used to study the octasaccharides bound to AT. The combined use of this solution with a higher temperature (35°C) than was used in the NMR study of AGA*IA pentasaccharide / AT complex [8] was necessary to increase the dissociation constants (from nM to μM). This achieved faster exchange conditions between octasaccharide and AT with respect to NMR timescales, as required for the analysis of the complex. Optimum tr-NOEs were observed with the lowest ligand:protein ratio [11]. However, owing to the difference between protein and oligosaccharide molecular weight, only high ligand:protein molar ratios (10:1 up to 20:1) could usually be analysed. The increased sensitivity available with cryoprobe technology allowed the ratio of ligand to octasaccharide:AT to be reduced to a molar ratio of 3.5:1.

Characterization and conformational analysis of free octasaccharides

Octasaccharides **A** and **B** (Figures 2 and 3) were obtained by combining ATIII affinity chromatography and CTA-SAX anion exchange chromatography on a semi-preparative scale, starting from octasaccharide GPC fractions of enoxaparin, as described in the experimental section. ^1H resonances were assigned by two dimensional (2D) NMR homonuclear spectra (DQF-COSY and TOCSY, data not shown). NOESY experiments were performed to sequentially connect the saccharide ring systems. Proton resonances of the octasaccharides **A** and **B** (Table 1) agreed with

the proposed structure, in which the active pentasaccharide AGA*IA is located at the non-reducing and reducing end respectively.

The conformation of the free octasaccharides were analysed by three bond proton-proton coupling constants ($^3J_{H-H}$) and NOEs. $^3J_{H-H}$ couplings measured by one-dimensional ^1H spectra indicated that all glucosamine residues were present in aqueous solution in the $^4C_1$ conformation. In fact, the small $^3J_{H1-H2}$ (3.4-3.6 Hz) and the large $^3J_{H2-H3}$ (10-11 Hz) values indicated an axial-equatorial relationship between H1 and H2 and trans-diaxial relationship between H2 and H3, respectively. Since all measured coupling constants are typical for the $^4C_1$ of glucosamine conformation in neutral aqueous solutions, it can be concluded that neither the adjacent residues nor the ionic strength (0.6M NaCl) used in the experiments influence the conformation of this residue. In contrast, the conformations of ΔU and ΔU_{2S} are influenced by 2-O-sulfation. The measured values of $^3J_{H1-H2}$ and $^3J_{H3-H4}$ of 6.0 Hz and 3.7 Hz respectively, are consistent with a preferred $^2H_1$ half-chair conformation for the ΔU residue of octasaccharide **A**, whereas values of $^3J_{H1-H2}$ and $^3J_{H3-H4}$ of 3.0 Hz and 4.8 Hz respectively, indicate a preferred $^1H_2$ half-chair conformation for the ΔU_{2S} residue of octasaccharide **B** [28]. Only $^3J_{H1-H2}$ and $^3J_{H4-H5}$ could be used to analyse the conformational equilibrium of such residues because of strong coupling effects due to the overlapping of H2 and H3 signals of $IdoA_{2S}$ residues. The iduronic acid within the AGA*IA sequence in both octasaccharides **A** and **B,** as well as the sulfated iduronate external to AGA*IA in octasaccharide **A,** showed $^3J_{H1-H2}$ and $^3J_{H4-H5}$ values compatible with the presence of both $^1C_4$ and $^2S_0$ conformations. On the other hand, the non-sulfated iduronic acid residue preceding the AGA*IA sequence in octasaccharide **B** shows smaller $^3J_{H1-H2}$ and $^3J_{H5-H4}$ values, indicating a predominant $^1C_4$ conformation (>90%) (Table 2). These data are supported by intra-residue NOE measurements (Table 3). Since $^1C_4$ and $^2S_0$ conformations exhibit distinct H5-H2 distances (0.4nm and 0.24nm, respectively) (Fig. 1) [13], the corresponding NOE effects can be considered as a marker for the $^2S_0$ conformation. Particularly, the ratio between H5-H4 (showing the same distance in both $^1C_4$ and $^2S_0$ geometries) and H5-H2 NOEs, can be related to the percentage of the two conformers. A weak I5-I2 NOE value, not compatible with a pure $^1C_4$ conformation, was measured for $IdoA_{2S}$* in both octasaccharides, indicating that this residue is in equilibrium with the $^2S_0$ form (Fig. 4a and 4c). Nevertheless, such a magnitude is much smaller than the corresponding NOE measured on $IdoA_{2S}$ of the AGA*IA sequence in water solution, characterized by a $^1C_4$:$^2S_0$ ratio of 40:60. This finding indicates a shift of the equilibrium toward the $^1C_4$ conformation in high ionic strength solution [15]. The lack of an H5-H2 NOE in the non-sulfated IdoA residue of octasaccharide **B** indicates that only the $^1C_4$ conformation is adopted, in agreement with the coupling constant results (Fig. 4c).

Conformational analysis of bound octasaccharides.

The anomeric region expansions of ^{1}H-NMR spectra of octasaccharide **A** and **B** measured at 600 MHz in the presence of AT are shown in figures 2 and 3, respectively, in comparison with proton spectra in the free state. The small shifts of the proton resonances and the increased linewidth, arising from the higher correlation time induced by protein binding, indicate the occurrence of an interaction between the octasaccharides and AT in an equilibrium regulated by intermediate dynamic exchange. Notably, the increased line broadening observed for the trisulfated glucosamine signal indicates a strong interaction of this moiety with AT, confirming its relevance in the binding [29]. The evidence of the intermolecular interaction was supported by the increased NOE magnitudes induced by AT (Table 3).

The increased line-width compared to the free ligands and the presence of AT signals, rendered only the glucosamine $^{3}J_{H1\text{-}H2}$ couplings detectable. As expected, such coupling constants essentially have the same values as those measured in free octasaccharides (3.5-3.8 Hz), indicating that the $^{4}C_{1}$ glucosamine conformation is not affected by binding to AT. Iduronic acid conformations were investigated by quantitative analysis of tr-NOESY spectra, recorded using three different mixing times (100, 200, and 300 ms) (Table 3). In both octasaccharides **A** and **B**, a significant enhancement of the ratio between H5-H2 and H5-H4 NOE magnitudes of $IdoA_{2S}$*, with respect to the free-state was observed. The same enhancement was detected for the IdoA residue in octasaccharide **B**, whereas in octasaccharide **A**, $IdoA_{2S}$ did not show any I5-I2 NOE interaction (Fig. 4b and 4d).

These results suggest that the $IdoA_{2S}$* conformation is driven towards the $^{2}S_{0}$ form upon binding to AT, as observed in all heparin/AT complexes so far described, supporting the idea that binding between AT and AGA*IA extended oligomers is regulated by the same specificity found in AGA*IA/AT complexes [6, 8]. On the other hand, binding to AT appears to drive IdoA and $IdoA_{2S}$ towards $^{2}S_{0}$ and $^{1}C_{4}$ conformations, respectively. As expected, in the free-state, the $IdoA_{2S}$ moiety is in equilibrium between the $^{2}S_{0}$ and the $^{1}C_{4}$ (with a prevalence of the latter form). The interaction of octasaccharide **A** with AT drives these residues towards the $^{1}C_{4}$ conformation. In contrast, the $^{1}C_{4}$ conformation of IdoA of octasaccharide **B** is completely reversed to $^{2}S_{0}$ by the presence of AT. Such a result is particularly surprising since to our knowledge this is the first observation of non-

sulfated iduronic acid units adopting almost exclusively the $^{2}S_{0}$ conformation in heparin or heparin oligomer / protein complexes.

Docking studies In order to localize octasaccharides **A** and **B** in the AT binding site, preliminary docking studies were carried out by using the AutoDock program. All **A** and **B** octasaccharide models were created by Macromodel version 7.1 starting from previously reported models [8, 12]. To evaluate the ability of our theoretical structures to interpret experimental data with regard to the conformation adopted by IdoA and $IdoA_{2S}$ moieties, two models were used for each molecule; setting the conformation of the iduronate residue in one such unit to $^{1}C_{4}$ and the other to $^{2}S_{0}$ conformations. In all models, glucosamine residues were in the $^{4}C_{1}$ form, whereas, to avoid distortions of uronic acid ring, $IdoA_{2S}$* was fixed in the $^{2}S_{0}$ conformation. ΔU residues in octasaccharide **A** and ΔU_{2S} in octasaccharide **B** were fixed in $^{2}H_{1}$ and $^{1}H_{2}$ conformations respectively [28]. Glycosidic torsion angles were set according to published values [8, 12, 28] and structures were minimized while constraining H1-H3, H1-H4 inter-residue distances on the basis of values extrapolated from experimental NOE magnitudes.

In models of octasaccharide **B** with IdoA in $^{2}S_{0}$ and $^{1}C_{4}$ conformations, those structures giving the best scores by AutoDock simulations, as well as the majority of the conformations generated, were oriented to maintain the original AGA*IA contacts (Figure 5 and Table 4). In both of these models, the sulfate group of $IdoA_{2S}$* did not show any dipolar interaction with AT, similar to that observed for the AGAIA pentasaccharide [8]. In the model having IdoA in $^{1}C_{4}$ conformation, the octasaccharide non-reducing portion was spread out from the protein surface. In the other model, the $^{2}S_{0}$ conformation of IdoA drives the non-reducing end towards the protein surface, promoting polar contacts with Lys-136, Arg-132, Lys-133. Such additional interactions are identical to those occurring between AT and AGA*IA containing oligomers longer than a pentasaccharide [30]. These findings support NMR results indicating that, in octasaccaride **B** bound to AT, IdoA preceding the AGA*IA sequence adopts the $^{2}S_{0}$ conformation.

In octasaccharide **A,** some of the conformations predicted by docking simulations maintain the original AGA*IA positioning, while others were shifted to preserve the placement of the reducing end residues; others showed inverted orientations. In the output ensemble of such simulations no predominant conformation can be found, either in terms of score, or with regard to cluster

populations. Moreover, in terms of ligand-protein polar contacts, no significant differences were observed between docked structures having $IdoA_{2S}$ in $^{1}C_4$ and $^{2}S_0$.

In agreement with these findings, Belzar et al. [22] indicated two possible orientations for a reducing-end extended AGA*IA containing heptasaccharide bound to AT; one maintaining the original AGA*IA positioning and the other shifted along the AT binding site to preserve the placement of the reducing end residues. It is noteworthy that extension of both the above heptasaccharide and octasaccharide **A** with a disaccharide did not show any dipolar interaction with AT when AGA*IA maintained its original docking position. This binding mode is thought unfavourable, at least at low ionic strength. At the same time, "shifted orientations" lack dipolar contacts between A* 3-O-sulfated group and AT, which are considered essential in heparin-AT interactions [29]. Since the results of docking studies do not allow us to differentiate between these two modes of binding, we are planning to perform a comparison between experimental trNOEs and theoretical trNOEs computed using the CORCEMA program on the different conformations [8].

CONCLUSION.

Docking calculations suggest a possible role of the extension towards the non-reducing end of octasaccharide **B**. The polar contacts with Lys-136, Arg-132, Lys-133, which are not part of the pentasaccharide binding region of AT, principally occur when IdoA is in the $^{2}S_0$ conformation, supporting previous experimental evidence (30). The role of the extension towards the reducing end of octasaccharide **A** is less clear. This region may actively contribute to increase the contact with the protein only if the octasaccharide is shifted by one disaccharide unit toward the "top" of helix D of AT. However, in this binding mode, the 3-O-sulfate group of A*, which is considered essential for the interaction, is not involved in any polar interaction with AT. The relatively strong increase in line width observed for the anomeric proton of A* in the bound state (Figures 1 and 2), suggests a tight interaction between this residue and AT and is not compatible with this hypothesis. An in-depth analysis of tr-NOEs and comparison with theoretical tr-NOEs computed on different docked conformations is required to define the correct structure of the oligosaccharides in the complex. The complete reversal of conformation (from $^{1}C_4$ to $^{2}S_0$) observed for the non-sulfated iduronate residue preceding the AGA*IA sequence in octasaccharide **B** raises the question of whether such a conformational transition actually modulates the interaction of the active pentasaccharide with AT. In fact, although such an IdoA residue is invariably present in all chains of porcine mucosal heparin with high affinity for AT, it has been shown that it is not essential for

high affinity binding to AT [23]. In order to throw light on this important aspect, a detailed comparison of 3D structures in the AT-bound state and the corresponding affinities for AT of variants of AGA*IA sequences preceded by different uronic acid residues will be required.

ACKNOWLEDGEMENTS

M.G., S.G., D.B., and G.T. thank Sanofi-Aventis and the Ronzoni Foundation for financial support. S.G. also thanks prof. Kenneth M. Merz Jr. and his group for the helpful training in docking procedures.

REFERENCES

1. Casu, B., (2005) Structure and active domains of heparin. In Chemistry and Biology of Heparin and Heparan Sulphate. (Garg, H.G., Linhardt, R.J. and Hales, C.A. ed.), pp. 1-28, Elsevier Ltd.
2. Casu, B. and Lindahl, U. (2001) Structure and biological interactions of heparin and heparan sulphate. Adv. Carbohydr. Chem. Biochem. ***57,*** 159-206.
3. Huntington, J.A. (2005) Heparin activation of serpins. In Chemistry and Biology of Heparin and Heparan Sulphate. (Garg, H.G., Linhardt, R.J. and Hales, C.A. ed.), pp 367-398, Elsevier Ltd..
4. van Boeckel, C.A.A., Grootenhuis, P.D.J. and Visser, A. (1994) A mechanism for heparin-induced potentiation of antithrombin III. Nat. Struct. Biol. **1**, 423-425
5. Petitou, M. and van Boeckel, C. A. A. (2004) A synthetic antithrombin III binding pentasaccharide is a new a drug! What comes next? Angew. Chem. Int. Ed. **43,** 3118-3133.
6. Jin, L., Abrahams, J.P., Skinner, R., Petitou, M., Pike, R. N. and Carrell, R. W. (1997) The anticoagulant activation of antithrombin by heparin. Proc. Natl. Acad. Sci. U.S.A. **94**, 14683-14688.
7. Skinner, R., Abrahams, J.P., Whisstock, J.C., Lesk, A.M., Carrell, R.W. and Wardell, M.R. (1997) The 2.6 Å structure of antithrombin indicates a conformational change at the heparin binding site. J. Mol. Biol. **266**, 601-609.
8. Hricovini, M., Guerrini, M., Bisio, A., Torri, G., Petitou, M. and Casu, B. (2001) Conformation of heparin pentasaccharide bound to antithrombin III. Biochem. J. **359**, 265-272.
9. Poveda, A. and Barbero J.J. (1998) NMR studies of carbohydrate protein interactions in solution. Chem. Soc. Rev. **27**, 133-143.

10. Hricovíni, M., Nieto P.N. and Torri, G. (2002) NMR of sulfated oligo and polysaccharides. In NMR of Glycoconjugates. (Barbero, J.J. and Peters T. ed.), pp. 189-223. Wiley-VCH, Weinheim, Germany.
11. Carlomagno T. (2005) Ligand-target interaction: what we can learn from NMR? Annu. Rev. Biophys. Biomol. Struct. **34,** 245-266.
12. Mulloy, B., Forster, M.J., Jones, C. and Davies, D.B. (1993) NMR molecular modelling studies of the solution conformation of heparin. Biochem. J. **293,** 849-858.
13. Ragazzi, M., Ferro, D.M. and Provasoli, M. (1986) A force-field study of the conformational characteristics of the iduronate rings. J. Comp. Chem. **7,** 105-112.
14. Ferro, D.R., Provasoli, A., Ragazzi, M., Torri, G., Casu, B., Gatti, G., Jacquinet, J.C., Sinay, P., Petitou, M. and Choay. J. (1986) Evidence for conformational equilibrium of the sulfated L-iduronate residue in heparin and in synthetic heparin mono-and oligosaccharides: NMR and force-field studies. J. Am. Chem. Soc. **108**, 6773-6778.
15. Ferro, D., Ragazzi, M., Provasoli, A., Perly, B., Torri, G., Casu, B., Petitou, M., Sinaÿ, P. and Choay, J. (1990) Conformers population of L-iduronic acid residues in glycosaminoglycan sequences. Carbohydr. Res. **195,** 157-167
16. Mulloy B. and Forster M. J. (2000) Conformation and dynamics of heparin and heparan sulfate. Glycobiology. **10**, 1147-1156.
17. Casu, B., Guerrini, M. and Torri, G. (2004) Structural and conformational aspects of the anticoagulant and antithrombotic activity of heparin and dermatan sulphate. Curr. Pharm. Des. **10,** 939-949.
18. Casu, B., Petitou, M., Provasoli, M., Sinay, P. (1988) Conformational flexibility: a new concept for explaining binding and biological properties of iduronic acid-containing glycosaminoglycans. Trends Biochem. Sci. **13**, 221-225.
19. Raman, R., Sasisekharan, V. and Sasisekharan, R., (2005) Structural insights into review biological roles of protein-glycosaminoglycan interactions. Chem. & Biol. **12,** 267–277.
20. Sundaram, M., Qi, Y., Shriver, Z., Liu, D., Zhao, G., Venkataraman, G., Langer, R. and Sasisekharan, R. (2003) Rational design of low-molecular weight heparins with improved *in vivo* activity. Proc. Natl. Acad. Sci. U.S.A. **100,** 651-656.
21. Olson, S.T., Bjork, I., Sheffer, R., Craig, P.A., Shore, J.D. and Choay, J.(1992) Role of the antithrombin-binding pentasaccharide in heparin acceleration of antithrombin-proteinase reactions. J. Biol. Chem. **267,** 12528-12538.

22. Belzar, K.J., Dafforn, T.R., Petitou, M., Carrell, R.W. and Huntington, J.A. (2002) The effect of a reducing-end extension on pentasaccharide binding by antithrombin. J. Biol. Chem. **275,** 8733-8741.
23. Thunberg, L., Bäckström, G. and Lindahl, U. (1982) Further characterization of the antithrombin-binding sequence in heparin. Carbohydr. Res. **100**, 393-410.
24. Morris, G.M., Goodsell, D.S., Halliday, R.S., Huey, R., Hart, W.E., Belew, R.K. and Olson A.J. (1998) Automated docking using a lamarckian genetic algorithm and an empirical binding free energy function. J. Comput. Chem. **19,** 1639-1662.
25. Hook M. Bjork I. Hopwood J. Lindahl U. (1976) Anticoagulant activity of heparin: separation of high-activity and low-activity heparin species by affinity chromatography on immobilized antithrombin. FEBS Letters. **66**(1), 90-3.
26. Mourier, P.A.J. and Viskov, C. (2004) Chromatographic analysis and sequencing approach of heparin oligosaccharides using cetyltrimethylammonium dynamically coated stationary phases. Analytical Biochem. **332,** 299-313.
27. Wang, B., Raha, K., Liao, N., Peters, M. B., Kim, H., Westerhoff, L M., Wollacott, A.M., Van der Vaart, A., Gogonea, V., Suarez, D., Dixon, S.L., Vincent, J.J., Brothers, E.N. and Merz K.M.Jr. (2005) DivCon 4.x, distributed by QuantumBio Inc., State College, PA 16803.
28. Ragazzi, M., Ferro, D.R., Provasoli, A., Pumilia, P., Cassinari, A., Torri, G., Guerrini, M., Casu, B., Nader, H.B. and Dietrich. C.P.(1993) Conformation of the unsaturated uronic acid residues of glycosaminoglycan disaccharides. J. Carbohydr. Chem. **12,** 523-535.
29. Petitou, M, Casu, B. and Lindahl U. (2003) 1976-1983, a critical period in the history of heparin: the discovery of the anti thrombin binding site. Biochimie. **85,** 83-89.
30. Arocas, V., Boris, T., Bock, S.C., Olson, S.T. and Bjork, I. (2000) The region of antithrombin interacting with full-length heparin chains outside the high-affinity pentasaccharide sequence extends to lys 136 but not to lys 139. Biochemistry **39,** 8512-8518.

Table 1a 600MHz proton chemical shifts of octasaccharide **A** residue measured at 308K.

	ΔU	**$GlcN_{NAc,6S}$**	**GlcA**	**$GlcN_{NS,3,6S}$**	**$IdoA_{2S}$***	**$GlcN_{NS,6S}$**	**$IdoA_{2S}$**	**$GlcN_{NS,6S}$**
H1	5.223	5.463	4.665	5.526	5.261	5.451	5.290	5.494
H2	3.884	4.013	3.436	3.508	4.394	3.344	4.385	3.322
H3	4.293	3.860	3.754	4.436	4.238	3.728	4.261	3.763
H4	5.885	3.897	3.850	4.022	4.188	3.832	4.163	3.786
H5		4.096	3.825	4.198	4.861	4.080	4.832	4.185
H6a		4.493		4.537		4.493		4.424
H6b		4.260		4.320		4.321		4.364

Table 1b 600MHz proton chemical shifts of octasaccharide **B** residue.

	ΔU_{2S}	**$GlcN_{NS,6S}$**	**IdoA**	**$GlcN_{NAc,6S}$**	**GlcA**	**$GlcN_{NS,3,6S}$**	**$IdoA_{2S}$***	**$GlcN_{NS,6S}$**
H1	5.554	5.393	5.059	5.430	4.670	5.546	5.250	5.497
H2	4.675	3.329	3.832	3.976	3.437	3.507	4.373	3.316
H3	4.377	3.689	4.176	3.806	3.755	4.428	4.231	3.751
H4	6.044	3.881	4.120	3.805	3.842	4.026	4.201	3.823
H5		4.027	4.826	4.068	3.848	4.205	4.821	4.169
H6a		4.411		4.380		4.530		4.466
H6b		4.26		4.28		4.313		3.55

Table 2 $^{3}J_{H-H}$ coupling constants of IdoA , $IdoA_{2S}$ and $IdoA_{2S}$* residues of octasaccharides **A** and octasaccharides **B** measured in buffer solution.

$^{3}J_{H-H}$ (Hz)	Octasaccharide **A**	Octasaccharide **B**
IdoA		
$^{3}J_{H1-H2}$		1.9
$^{3}J_{H4-H5}$		2.5
$IdoA_{2S}$*		
$^{3}J_{H1-H2}$	3.4	3.8
$^{3}J_{H4-H5}$	3.1	3.1
$IdoA_{2S}$		
$^{3}J_{H1-H2}$	3.0	
$^{3}J_{H4-H5}$	2.8	

Table 3 H5-H2 and H5-H4 NOE magnitudes (%) of iduronic acid residues of octasaccharide **A** and **B,** in their free state and in the bound form, measured in buffer solution.

		OctasaccharideA		**OctasaccharideB**	
	Mixing (ms)	free ligand	bound ligand	Free ligand	bound ligand
H5-H2 IdoA	100			0	2.4
	200			0	4.5
	300			0	5.1
H5-H4 IdoA	100			2.6	4.0
	200			6.1	9.2
	300			7.2	10.8
H5-H2 $IdoA_{2S}$*	100	0	3.5	0	3.0
	200	0.9	7.0	0.4	7.8
	300	1.7	11.4	1.8	8.4
H5-H4 $IdoA_{2S}$*	100	1.9	3.4	2.9	4.1
	200	4.8	7.1	5.5	8.3
	300	7.2	10.4	8.1	12.2
H5-H2 $IdoA_{2S}$	100	0	0		
	200	0.4	0		
	300	1.8	0.9		
H5-H4 $IdoA_{2S}$	100	1.9	2.5		
	200	3.2	6.2		
	300	5.5	9.5		

Table 4 Polar contacts detected using the pentasaccharide /AT X-ray structure [6] and the octasaccaride **B**/AT (best scored docking output structures) complexes. Interactions were assumed to occur between ligand-protein polar groups closer than 6 Å. Listed contacts are referred to the best scored conformers predicted by AutoDock. The AGA*IA sequence is shown in bold.

[§] weak interactions: distance ≈ 8 Å

			Octasaccharide **B**	
Residue	Polar Group	AGA*IA x-ray structure [6]	IdoA $^2S_0$	IdoA $^1C_4$
ΔU_{2S}	COO		Lys 136[§]	
$GlcN_{NS,6S}$	NS		Arg 132 Lys 133	Arg 132
IdoA				
$GlcN_{NS,6S}$	6S	Lys 125 Arg 129	Lys 125 Arg 132	Lys 125 Arg 132
GlcA	COO	Lys 11 Asn 45 Lys 125	Lys 11 Asn 45 Lys 125	Lys 11 Asn 45 Lys 125
$GlcN_{NS,3,6S}$	NS 3S	Arg 13 Lys 114 Lys114	Arg 13 Lys 114 Lys 114	Arg 13 Lys 114 Lys 114
$IdoA_{2S}$*	COO	Arg47 Lys114	Arg 47 Lys 114	Arg 47 Lys 114
$GlcN_{NS,6S}$	NS 3S	Arg46 Arg47 Arg46 Arg47	Arg 46 Arg 47	Arg 46 Arg 47

Figure legends:

Figure 1 Scheme of $^{4}C_{1}$, $^{2}S_{0}$ and $^{1}C_{4}$ forms of the $IdoA_{2S}$ residue with the distances between H2 and H5.

Figure 2 Anomeric region of ^{1}H-NMR spectra (600 MHz) of octasaccharide **A** in 10 mM phosphate buffer (0.6 M NaCl, pH 7.4) at 35° C. $GlcN_{NS,6S}$red indicates reducing glucosamine (**a**). Complexed with AT (octasaccharide A/AT, 3.5:1) (**b**). Structure of the octasaccharide **A**, AGA*IA sequence is highlighted in the dashed frame (**c**).

Figure 3 Anomeric region of ^{1}H-NMR spectra (600 MHz) of octasaccharide **B** in 10 mM phosphate buffer (0.6 M NaCl, pH 7.4) at 35° C. $GlcN_{NS,6S}$red indicates reducing glucosamine. (**a**) In complex with AT (octasaccharide B/AT, 3.5:1) (**b**). Structure of the octasaccharide **B**, AGA*IA sequence is highlighted in dashed frame (**c**).

Figure 4 Iduronic acid residues region of the 2D- NOESY spectrum of the octasaccharide **A** (**a**) and octasaccharide **B** (**c**). Iduronic acid residues region of the transferred NOESY spectrum of the octasaccharide **A**/AT (**b**) and octasaccharide **B**/AT (**d**) 3.5:1 complexes. All spectra were measured at 35° C in 10 mM phosphate buffer, 0.6 M NaCl, pH 7.4 (mixing time: 200ms)

Figure 5 Best scored docking output structures of Enoxaparin octasaccharide **B** / AT complexes bearing IdoA in $^{1}C_{4}$ (cyan) and $^{2}S_{0}$ (blue) form. Structure of AGA*IA pentasaccharide extracted from X-ray AGA*IA / AT complex [6] was superimposed (wheat). In octasaccharide model with $^{1}C_{4}$ form, the reducing portion is spread out from the protein surface, whereas, in the other model, $^{2}S_{0}$ conformation of IdoA drives the non reducing end toward the protein surface promoting additional polar contacts.

Fig. 1

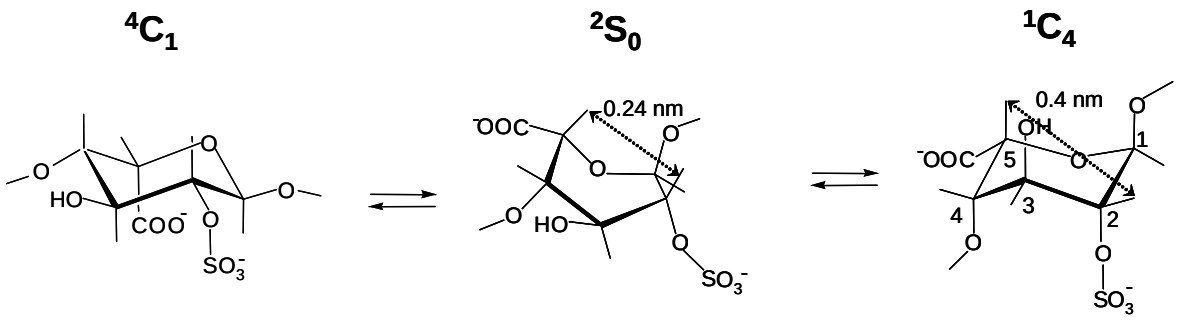

Fig. 2

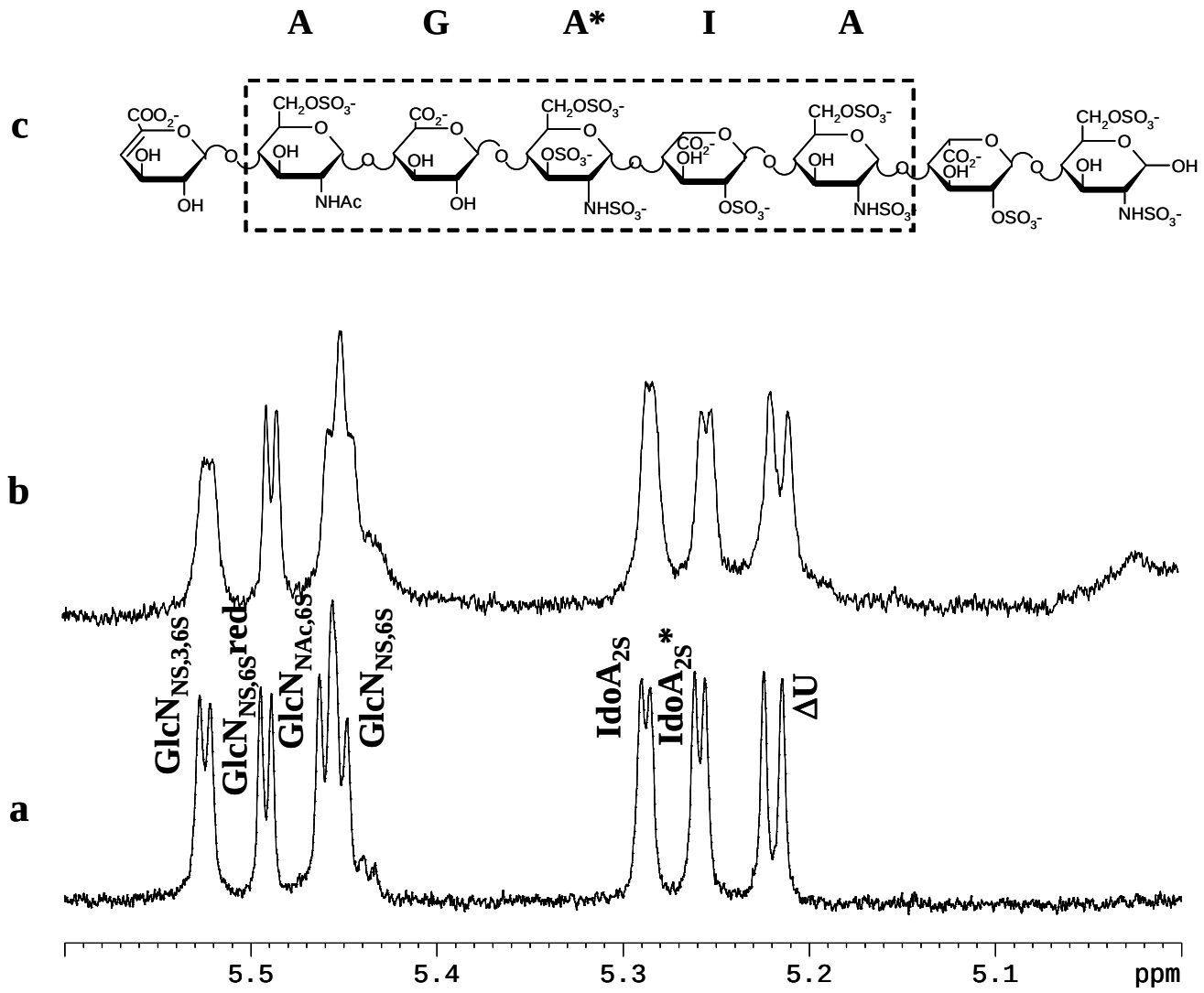

Fig. 3

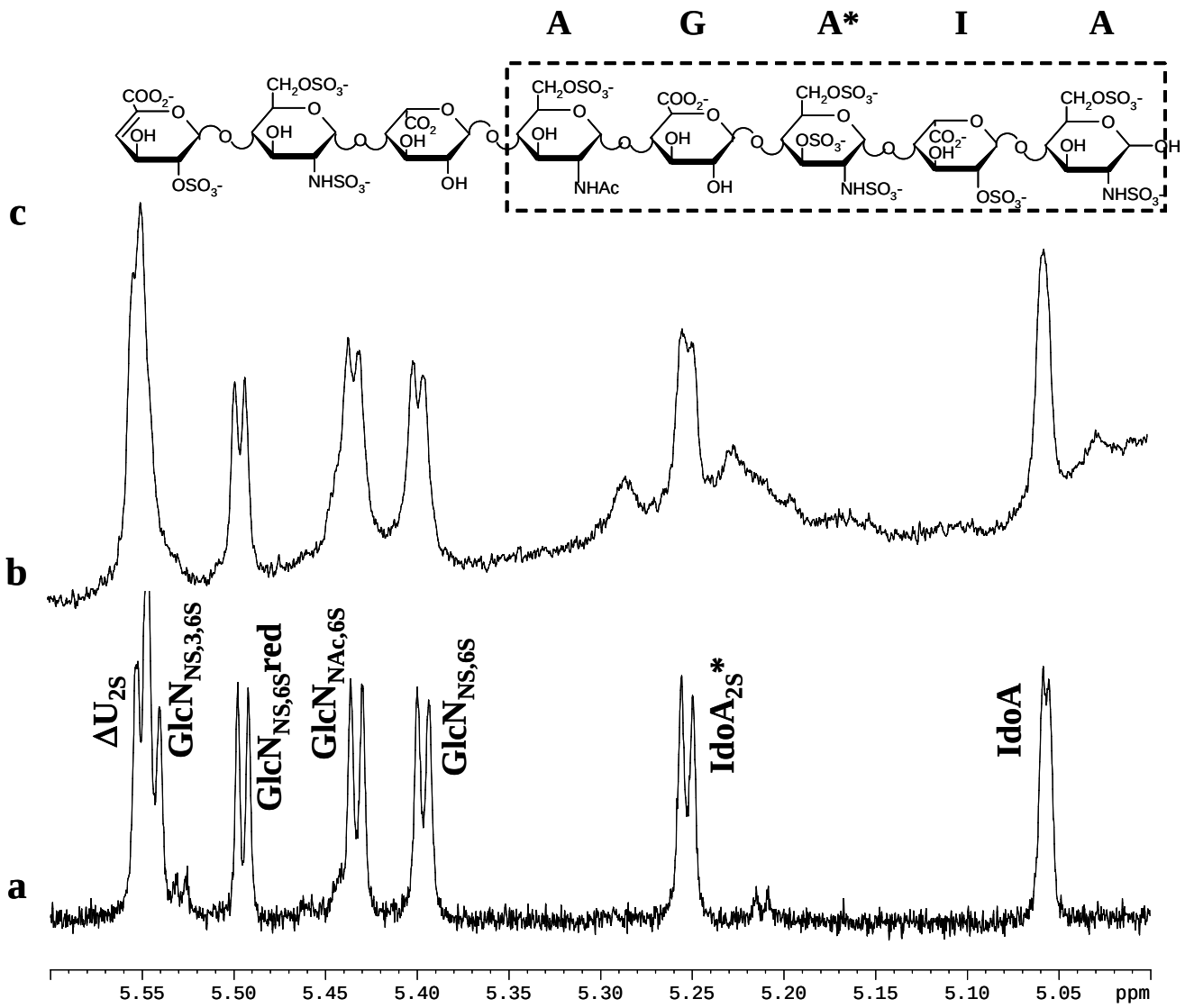

Fig. 4

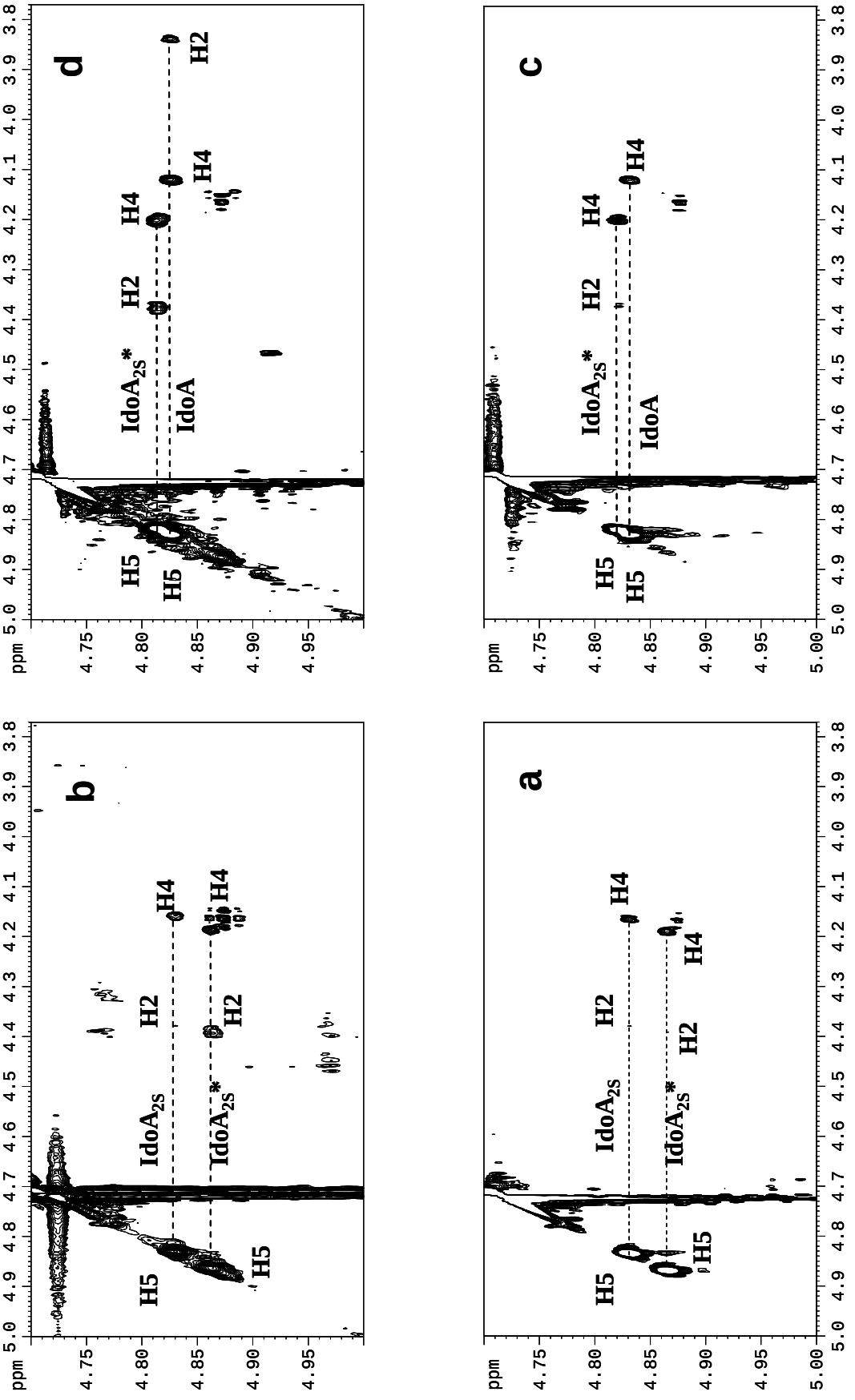

Fig. 5